A PORE-SCALE HYDRO-MECHANICAL COUPLED MODEL FOR GEOMATERIALS

E. CATALANO[*], B. CHAREYRE[*], A. CORTIS[†] AND E. BARTHELEMY [††]

[*]Grenoble INP, UJF Grenoble I, CNRS UMR 5521, 3SR lab
BP53, 38041 Grenoble Cedex 9, France
e-mail: catalano@hmg.inpg.fr
web: www.3s-r.hmg.inpg.fr/3sr/

[†]Earth Sciences Division
Lawrence Berkeley National Laboratory
Berkeley, CA, 94806, U.S.A.

[††]Grenoble INP, UMR CNRS 5519, LEGI
BP 53, 38041 Grenoble Cedex 9, France

Key words: DEM, Fluid-solid coupling, Pore network, Consolidation

Abstract. We present a model for fluid-saturated granular media coupled flow and mechanical deformation. The fluid is assumed to be incompressible and the solid part is assumed to be a cohesive granular material. Forces exerted by the fluid in motion are determinated and applied to solid particles. We derive a finite volumes formulation of the flow problem and we couple it to a discrete element method (DEM) formulation of the solid deformation.

The ability of the algorithm to solve transient problems is tested by simulating an oedometer test on a soil sample. The numerical solution of our model is in good agreement with Terzaghi's analytical solution.

1 INTRODUCTION

Discrete element modelling is a tool to study the phenomena that take place at the scale of elementary components of materials. Such a technique is of great interest when applied to geomechanics problems. Modelling the hydro-mechanical coupled response of saturated porous media is indeed one of the main topics of rock and soil mechanics, and inspired one of the main contributions of Karl Von Terzaghi, whose theory of consolidation of soils "[..]has been one of the strongest incentives in the creation of a science of soil mechanics. (M.A.Biot)". The model presented in this work aims at providing an effective tool for the analysis of the mutual influence between internal flow and deformation in geomaterials,

by modelling the interactions that take place at the particles scale. Depending on the type of problem, various strategies can be adopted for coupling the solid-fluid interaction, which differ essentially on how the fluid phase is being modelled.

At the microscopic (sub-pore) scale, the solid and fluid phases occupy different portion of the spatial domain and interact at their common interface. Thus, the microscopic fields which describe the properties of costituents may be considered as continua within a single phase, while exhibit discontinuities at the interfaces between phases. At such scale, fluid flow is governed by Stokes equations, which express fluid mass and moment conservation at small Reynolds and Stokes numbers

$$\nabla p = \mu \nabla^2 \mathbf{u} - \rho \nabla \Phi \tag{1}$$

$$\nabla \cdot u = 0 \tag{2}$$

where $\mathbf{u}$, and p are the microscopic fluid velocity and piezometric pressure, respectively, μ is the fluid dynamic viscosity, and Φ is a potential field (e.g., gravitational field). The piezometric pressure p is related to the absolute pressure p^* via $p = p^* - \rho \Phi$. A no-slip boundary condition for the fluid velocity at the grain boundaries is specified, $u = 0$, which is essentially responsible for the microscopic viscous energy losses (drag) that translate in a net loss of the macroscopic piezometric pressure, p, over the length of a porous column. The numerical solution of Stokes equations in spheres assemblies is computationally expensive, especially for complex three-dimensional pore geometries. Finite Element Methods (FEMs) [13] or Lattice-Boltzmann (LB) [14] methods follow a microscopical approach but often find limitations (on the problem size, i.e.) linked to a heavy demand in terms of computer memory and computational cost.

The continuum approach is often adopted at the macroscopic level when modelling the fluid phase in order to get acceptable computational costs [8]. In such approach, there is no direct coupling at the local scale, and flow-induced forces on particles are defined as function of meso-scale averaged fluid velocity obtained from porosity-based estimations of the permeability. The use of phenomenological laws for the estimation of the permeability, however, limits severely the predictive power of these models, in conditions where parameter are poorly calibrated. Moreover the adoption of such approach does not allow the analysis of the individual particle behaviour, and so cannot be applied to problems whose nature is purely micromechanical, like strain localization or internal erosion.

The model we propose represents a middle way between the abovementioned approaches: the solid phase is characterized by a sphere packing DEM model, while the fluid phase moves through finite volumes in a pore network built upon a discretization of the spheres packing void space, referred hereafter as *"Pore scale Finite Volumes'* (PFV).

Pore network models are based on a simplified representation of porous media as a network of pore and throats. They have been primarily developed to predict permeability of materials [11],[9] or in modelling multiphase flow effects from microstructure geometry [10], [15], [6], provided an appropriate interpretation on how fluids are exchanged between

pores and how such fluxes interact with the solid grains. These aspects will be developed and discussed in what follows. The ability of the model to reproduce the consolidation process will be finally tested.

2 THE GRAINS

The Discrete Element Method (DEM), as it is implemented in the open-source code YADE [19], was used to model the mechanics of the solid phase. The approach is fully micromechanical, the soil behaviour being modelled by defining the mechanical properties of the interaction between the grains [5]. Here, the soil grain's shape is assumed to be spherical. This is a quiet usual assumption in DEM works, except in cases when the specific influence of the grain shape on the soil behaviour is under investigation. In other circumstances, use of polydisperse sphere packings is sufficient to reliably reproduce the soil behaviour [16].

At each DEM simulation time step, particles in contact are detected and then subjected to a repulsive force according to an elasto-plastic interaction law. The particles are then accelerated according to the second Newton's law of motion, and their position is updated for the next step. A detailed description of YADE DEM implementation in YADE is available in the code's documentation [20].

3 THE PORES

Delaunay triangulation and its dual Voronoi graph were used to discretize the void space and formulate the flow problem. Such geometrical representations are commonly used in soil mechanics for the definition of microscale stresses and strains [12] or in pore-scale modelling of single-phase or multi-phase flow [10]. The C++ library CGAL [17] is used for the triangulation procedure. Here, the generalization to weighted points of the Delaunay triangulation (*Regular Delaunay triangulation*) was adopted, where weights account for the radius of spheres [17]. A system of tetrahedra arises in a 3D framework, each one representing a pore (see fig.1(A) and fig.2). Such scheme constitutes a discretization of the void space in finite volumes, which will allow the approximation of the flow equations. The dual Voronoi diagram constitutes a network whose edges never cross non-void regions (see fig.1(B)) and form closed regions each one containing exactly one grain (coloured in fig.1(B)). Such network ideally represents the flow path of fluid within the porous sample and allows the formulation and resolution of the flow problem, as it will be detailed in the following.

4 FLUXES

The porous medium is assumed to be saturated with an incompressible fluid. For each tetrahedron of the triangulation, the volume of fluid coincides with the total volume Θ_i (see fig.2) which is not occupied by any portion of the spheres. As a consequence, the continuity equation for pore i, can be recast into a surface integral form using the
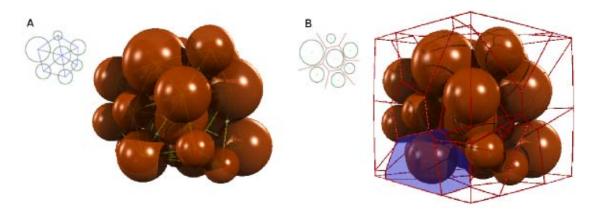
Figure 1: Regular Delaunay triangulation (A), Voronoi diagram (B)

divergence theorem,

$$\dot{V}_i^f = \int_{\partial \Theta_i} (\mathbf{u} - \mathbf{v}) \cdot \mathbf{n} ds \tag{3}$$

where the time derivative of the volume of fluid is obtained by integration over the pore contour $\partial \Theta_i$ ($\mathbf{n}$ its unit normal) of a relative fluid ($\mathbf{u}$) - contour ($\mathbf{v}$) velocity term. Dealing with tetrahedra, all geometrical quantities can be easily handled. Each pore i shares with its four neighbours $j_i \in \{j_1, j_2, j_3, j_4\}$ a triangular facet of surface S_{ij}. For each facet, it can be recognized a zone occupied by the solid portions of grains S_{ij}^s, a zone occupied by the fluid S_{ij}^f (see fig.2C), and the fluid - solid interface, where $(\mathbf{u} - \mathbf{v}) \cdot \mathbf{n} = 0$. The integration domain can therefore be restricted to S_{ij}^f and the equation (3) rewritten in a discrete form as a sum of the fluxes that each pore exchanges with its neighbours.

$$\dot{V}_i^f = \sum_{j=j_1}^{j_4} \int_{S_{ij}^f} (\mathbf{u}_n - \mathbf{v}_n) ds = \sum_{j=j_1}^{j_4} q_{ij} \tag{4}$$

4.1 Local Conductances

Our approach allows the definition of a local conductance k_{ij} between adjacent pores i and j and of an inter-pore gradient, defined as the ratio between the pressure drop $p_i - p_j$ and the length l_{ij}, the interpore distance. Based on the Voronoi diagram that was presented in previous sections, such length is assumed to be the euclidean distance between the Voronoi centres, labelled P_i and P_j in fig.2(D). The linear relation between the flux q_{ij} and the local pressure gradient, can be expressed as follows:

$$q_{ij} = k_{ij} \frac{p_i - p_j}{l_{ij}} \tag{5}$$

Assuming the flow as laminar viscous and incompressible, Hagen-Poiseuille equation represents the ideal physical framework by which local conductances may be interpreted.
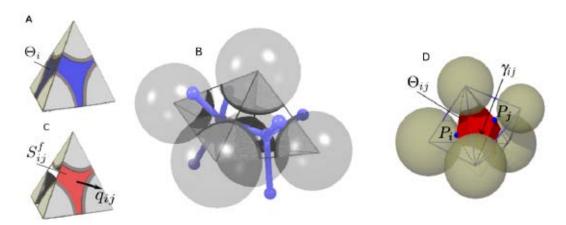
Figure 2: Volume of fluid in a pore (A), adjacent pores and local connections (B), fluid domain of pore contour (C), pore partition for hydraulic radius definition (D)

Considerable efforts have been devoted in the literature to the generalization of Poiseuille's law to pores of complex shape [7], and to the definition of a ngeneralized hydraulic radius [3]. By analogy with the Hagen-Poiseuille relation, k_{ij} may therefore be defined as follows:

$$k_{ij} = \alpha \frac{S_{ij}^f R_{ij}^{h\,2}}{\mu} \tag{6}$$

where α is a non-dimensional conductance factor which reflects the throat's shape. For $\alpha = 1/2$, Hagen-Poiseuille equation takes the classical form which can be obtained for circular shaped conduits. μ is the fluid dynamic viscosity. S_{ij}^f is the *fluid* domain of equation (4). The hydraulic radius R_{ij}^h is defined as the ratio between a volume filled with liquid and a wetted surface,

$$R_{ij}^h = \frac{Volume_{fluid}}{Surface_{wetted}} = \frac{\Theta_{ij}}{\gamma_{ij}} \tag{7}$$

for each pore connection, ij. As already seen in previous sections, neighbouring pores have three grains in common, and thus three vertices of the triangulation resulting in a triangular plane facet. Those three vertices, together with the Voronoi centres (P_i, P_j, see fig.2(D)) that are defined for the two pores, define a relevant pore partitioning and allow to access the total fluid volume Θ_{ij} and the wetted surface γ_{ij}, and the corresponding hydraulic radius (see fig.2(D)).

4.2 Forces

We will give very few details on the definition of forces exerted by the fluid to the solid particles. For a complete description on how the expressions that will be presented hereafter have been obtained, refer to Chareyre et al. [1].

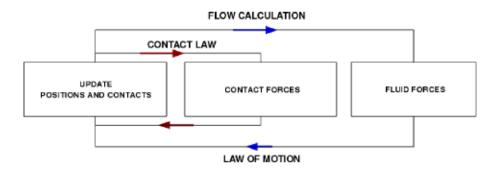The total force F^k on particle k can be defined as follows:

Figure 3: Coupled DEM-Flow computation cycle

$$F^k = \int_{\partial \Gamma_k} (p^* \mathbf{n} + \tau \mathbf{n}) ds \tag{8}$$

where $\partial \Gamma_k$ denotes the solid surface of the particle k, p^* the absolute pressure and τ the shear stress. As detailed in the introduction, the piezometric pressure p governing the flow problem is defined as $p = p^* - \rho \Phi(x)$. By this definition, the F^k term can be splitted in three components:

$$F^k = \int_{\partial \Gamma_k} \rho \Phi(x) \mathbf{n} ds + \int_{\partial \Gamma_k} p \mathbf{n} ds + \int_{\partial \Gamma_k} \tau \mathbf{n} ds = F^{b,k} + F^{p,k} + F^{v,k} \tag{9}$$

where $F^{b,k}$ denotes the buoyancy force, that can be computed indipendently, while $F^{p,k}$ and $F^{v,k}$ are those forces which result from viscous flow, respectively due to losses of piezometric pressure and to viscous shear stress.

5 PROBLEM SOLUTION

The resolution of the flow problem can now be integrated into the algorithm presented in section 2. Combining equations (4) and (5), we obtain:

$$\dot{V_i^f} = \sum_{j=j_1}^{j_4} q_{ij} = k_{ij} \frac{p_i - p_j}{l_{ij}} = K_{ij}(p_i - p_j) \tag{10}$$

At each cycle of computation, once the positions of the spheres are updated, new contacts are detected and the volumetric variation of pores is computed. The contact law and the fluid problem resolution give the contact forces and the *fluid* forces to be applied to particles, whose positions is again updated according to the law of motion (see fig.3). The matrix K_{ij} is sparse, symmetric and positive defined. The linear system is then solved by using an over-relaxed Gauss-Seidel algorithm.
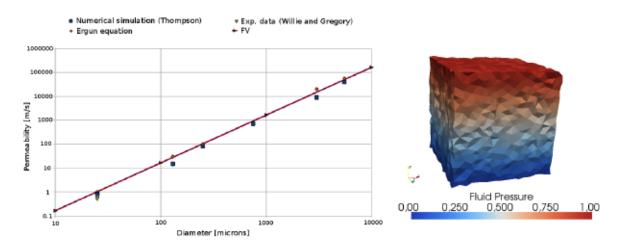
Figure 4: Predicted permeabilities. Comparison with experimental/analytical/numerical results (a). Pressure field (b).

6 PERMEABILITY MEASUREMENTS

The first tests that have been prepared to verify the relevance of the model implementation were based on the analysis of a flow trough a fixed solid skeleton ($\dot{V}_i^f = 0$ in eq.10). A pressure gradient was then applied to the granular sample. The flow boundary conditions are the ones shown in fig. 5: pressure is imposed on top and bottom boundaries, while a no-flux condition is imposed on lateral boundaries. Thus, on top and bottom boundaries the pressure was imposed and fixed ($p = 1$ and $p = 0$ respectively). Inlet Q_i and outlet Q_o flow rates can be then measured. It was found that $Q_i - Q_o < 10^6 \simeq 0$, which indicates a good convergence of the numerical solver. An estimation of a macroscopic *Darcy-like* permeability $[m^2]$ of the sample is then possible, being possible to assess the Darcy velocity of fluid flowing within the sample, $V_{Darcy} = Q/S$, with S the section of the sample and $Q = Q_i = Q_o$. Permeability can be thus estimated from the following relation:

$$K = \mu \frac{Q}{S} \frac{h_0}{\Delta p} \quad [m^2] \tag{11}$$

where h_0 is the height of the sample, Δp the pressure drop and μ the viscosity of the fluid. Figure 4(a) compares the assessed permeability values with experimental data by Willie and Gregory [18], the Ergun equation and numerical results obtained by Thompson [11]. Figure 4(b) shows the pressure field associated to the given boundary conditions.

Table 1 shows a comparison between the PFV solution with the solution obtained by small scale Stokes flow FEM computations in terms of degrees of freedom to compute the pressure field and CPU time for solving. It can be seen how in the case of PFV calculation, the total number of DOFs and CPU time required for calculating flow and forces acting on the particles are reduced drastically with respect to small scale Stokes flow FEM calculations. Not available values are relative to computations whose occupancy of

memory was out the computer's capacity. The pressure fields and effective permeabilities that were computed had been compared to FEM solutions and found in good agreement. For details, see Chareyre et al.[1].

Table 1: Comparison of DOF's and CPU time between FEM and PFV (one iteration).

Nb of spheres	FEM dof's	PFV dof's	FEM time [s]	PFV time [s]
9	1.7e5	45	300	0.00022
200	1.2e6	1093	5400	0.0046
2e3	not available (n.a.)	12e3	n.a.	0.091
2e4	n.a.	11e4	n.a.	2.21

7 MONODIMENSIONAL CONSOLIDATION

The ability of the algorithm to solve transient problems was finally tested by analyzing the consolidation process of a sample subjected to axial load. Grains are free to move, so the system to be solved is the one expressed in eq.(10). Boundary conditions are set in order to reproduce an oedometer test, as it will be detailed hereafter. The analysis of the evolution of settlement and excess pore pressure in space and time and the comparison of the numerical solution with the analytical solution obtained by Terzaghi in 1923 in his "*Theory of consolidation of soils*" will constitute a validation for the model.

7.1 The Terzaghi's analytical solution

The consolidation process is a classical hydro-mechanical problem. The mechanisms that govern the evolution of the deformation depend on a variation of effective stresses, coupled to processes of diffusion of the interstitial water. Such phenomenon depends therefore on the properties of the porous medium, like permeability and deformability, and on the problem geometry, defined by the boundary conditions and the drainage patterns which characterize the medium. The load applicated to a saturated medium is initially entirely carried by the fluid phase, as the water can not instantly flow out of the medium. An increase of pore pressure is induced, whose entity varies within the medium, while the external pressure keep a costant value u_0. A gradient of pressure is then established, resulting in a filtration flux whose duration depend on the medium properties. As the water progressively flows out of the medium, the load is transferred from to liquid to the solid phase, and the medium starts to deform. The process ends once the excess pore water pressure is fully dissipated.

The equation of monodimensional consolidation reads:

$$\frac{\partial u}{\partial t} = C_v \frac{\partial^2 u}{\partial z^2} \tag{12}$$

where u is the fluid pressure, z the height of the sample, C_v the consolidation coefficient, defined as follows:

$$C_v = \frac{K}{m_v g \rho_w} \tag{13}$$

where K is the permeability of the soil expressed in m/s, $m_v = \Delta\varepsilon_v/\Delta\sigma'_v$ the coefficient of volume compressibility, g the gravity acceleration and ρ_w the density of the fluid. Terzaghi's analytical solution is usually given in terms of consolidation degree U_z, defined as the ratio between the excess pore pressure at instant t and the initial one, and average degree of consolidation U_m, defined for a soil layer of heigth H as the ratio between the settlement S at the instant t, $(S(t) = \Delta H(t))$, and the final settlement S_c $(S_c = \Delta H_{final})$.

$$U_z = \frac{u(z,t)}{u_{max}} \tag{14}$$

$$U_m = \frac{S(t)}{S_c} \tag{15}$$

A non-dimensional time parameter is introduced, T_v, defined as:

$$T_v = \frac{C_v t}{L^2} \tag{16}$$

where t is the effective time, and L the longest drainage path of the generic fluid particle. $T_v = 0$ at the begin of consolidation, whereas $T_v = 1$ (100%) at the end of the process.

7.2 Numerical results

Setting up the simulation, boundary conditions were defined according to the oedometric conditions, which mirror the main hypothesis of Terzaghi's theory, briefly recalled hereafter: settlements and fluxes take place along one unique direction; the soil is homogenous and saturated; stress-strain relation is linear; the liquid and solid phase are incompressible; small and time-independent strains; validity of Darcy's Law. Boundary conditions are shown in figure 5. Lateral strains are imposed to be none ($\varepsilon_{xx} = \varepsilon_{yy} = 0$). A slip condition was set at the boundaries. Both upward and downward drainage ways were activated ($L = H/2$ in eq.16). A relative dense sample was created, to minimize the dispersion of pores' dimension and avoid strong heterogeneities within the sample. 5000 slightly polydispersed grains were employed to build a cubic sample ($l = 0.1m$) which was then subjected to an axial external load $\sigma_{ext} = 5kPa$. The external fluid pressure was set to be none, $u_0 = 0$.

The result that were obtained are shown in figure 6, with the evolution ef excess pore pressure (left diagram) which rose up to $5kPa$ ($= \sigma_{ext} = u_{max}$) and then gradually decreased. A good agreement is found in terms of evolution of settlement and excess of pore pressure. The central diagram shows the evolution of U_z, as defined in eq.14. The four curves are relative to four phases of the consolidation process, for $T_v = 0.0$ (0%
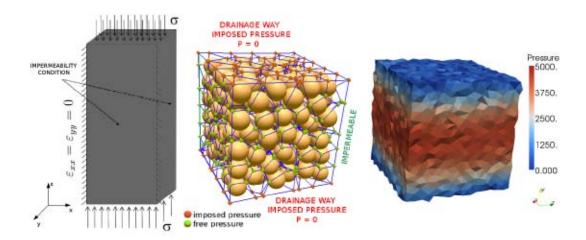
Figure 5: Boundary Conditions (left). Pressure field (10% of consolidation completed) (right).
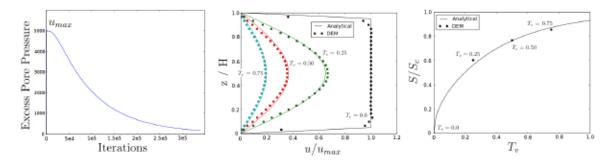

Figure 6: Oedometric Consolidation - Results obtained and comparison with Terzaghi solution

of consolidation completed), $T_v = 0.25$, $T_v = 0.50$, $T_v = 0.75$. The analytical solution (continued line) is compared to the numerical result (points) and found in good agreement. Similarly, the right curve shows the evolution of settlements.

8 CONCLUSIONS

We presented a pore-scale hydromechanical model for geomaterials that allows for a reliable and computationall efficient of the force exchange between fluid phase and solid particles, modeled a sphere packing. The pore-network model proved to be a relevant approach to interpret the physical phenomena that take place at the microscopic scale. The adoption of spherical grains assures an easy-to-handle pore geometry, and simplifies the derivation of local conductivities and *fluid* forces.

Comparison with small-scale Stokes flow FEM calculation shows how the CPU time required for solving the flow problem is drastically reduced by 6 orders of magnitude in our PFV-DEM approach. A good agreement has been found both in terms of pressure field and estimation of effective permeability. The ability of our approach to solve tran-

sient problems was tested by analyzing the consolidation process of a saturated sample subjected to axial load. The solution obtained is in good agreement with Terzaghi's analytical solution (both in time and space).

The application of the model to problems concerning internal erosion [2] and sediment transport in rivers are being tested. Current works focus on the reproduction of the liquefaction phenomenon as it takes place within a seabed under the action of natural ocean waves.

REFERENCES

[1] B. Chareyre, A. Cortis, E. Catalano, E. Barthélémy. Pore-scale Modeling of Viscous Flow and Induced Forces in Dense Sphere Packings. *(submitted)* (2011)

[2] H. Sari, B. Chareyre, E. Catalano, P. Philippe, E. Vincens. Investigation of internal erosion processes using a coupled DEM-Fluid method. *Particles 2011 II International Conference on Particle-Based Methods, E. Oate and D.R.J. Owen (Eds), Barcelona* (2011)

[3] Happel J., Brenner H. Low Reynolds Number Hydrodynamics. *Martinuis Nijhoff Publishers, Dordrecht* (1986)

[4] M.A. Biot. General theory of three dimensional consolidation. *Journal of Applied Physics* (1941) **12**:155–164.

[5] P.A. Cundall and O.D.L. Strack. A discrete numerical model for granular assemblies. *Geotechnique* (1979) **29**:47–65.

[6] R. R. O. Bonilla. Numerical simulation of undrained granular media. *PhD Thesis, University of Waterloo* (2004)

[7] Hilpert M.,Glantz R. and Miller C.T. Calibration of a Pore-Network Model by a Pore-Morphological Analysis. *Transport in Porous Media* (2003) **51**:267–285.

[8] M Zeghal and U El Shamy. A continuum-discrete hydromechanical analysis of granular deposit liquefaction *Int. J. Numer. Anal. Meth. Geomech.* (2004) **14**:(28)1361–1383.

[9] Bryant S. and Blunt M. Prediction of relative permeability in simple porous media. *Phys. Rev. A* (1992) **4**:(46)2004–2011.

[10] Steven Bryant and Anna Johnson. Wetting phase connectivity and irreducible saturation in simple granular media. *Journal of Colloid and Interface Science* (2003) **2**:(263)572–579.

[11] K. E. Thompson and H. S. Fogler. Modeling flow in disordered packed beds from pore-scale fluid mechanics. *AIChE Journal* (1997) **6**:(15)1377–1389.

[12] Katalin Bagi. Analysis of microstructural strain tensors for granular assemblies *International Journal of Solids and Structures* (2006) **43**:(10)3166–3184.

[13] R. Glowinski and T. W. Pan and T. I. Hesla and D. D. Joseph and J. Periaux. A Fictious Domain Approach to the Direct Numerical Simulation of Incompressible Viscous Flow past Moving Rigid Bodies: Application to Particulate Flow. *Journal of Computational Physics* (2001) **2**:(169)363–426.

[14] Han K., Feng Y.T., Owen D.R.J.Coupled Lattice-Boltzmann and discrete element modelling of fluid-particle interaction problems. *Computer and Structures* (2007) **85**:1080–1088

[15] Nordhaug H.F., Celia M., Dahle H.K. A pore network model for calculation of interfacial velocities. *Advances in Water Resources* (2003) **26**:1061–1074.

[16] Chareyre B., Modélisation du comportement d'ouvrages composites solgeosynthetique par élément discrets - Application aux ancrages en tranchées en tete de talus. *PhD Thesis, Université de Grenoble I - Joseph Fourier* (2003)

[17] Boissonnat J.D., Devillers O., Pion S., Teillaud M. and Yvinec M., Triangulations in CGAL *Computational Geometry: Theory and Applications* (2002) **22**:5–19

[18] Wyllie M.R.J., Gregory A.R., Fluid Flow trough Unconsolidated Porous Aggregates *Industrial and Engineering Chemistry* (1995) **47**:(7)1379-1388

[19] Smilauer V. and Chareyre B., Yade Dem Formulation. *Yade Documentation (V. Smilauer, ed.), The Yade Project, 1st ed.* (2010) (http://yade-dem.org/doc/formulation.html)

[20] V. Smilauer, E. Catalano, B. Chareyre, S. Dorofeenko, J. Duriez, A. Gladky, J. Kozicki, C. Modenese, L. Scholtes, L. Sibille, J. Stransky, and K. Thoeni. Yade Reference Documentation. *Yade Documentation (V. Smilauer, ed.), The Yade Project, 1st ed.* (2010) (http://yade-dem.org/doc/.)